Conf-9410314--1

UCRL-JC-119340
PREPRINT

Insights on the Local Density Approximation Plasma Polarization Shift as provided by the Optimum Potential Method

Brian Wilson
David A. Liberman

This paper was prepared for submittal to the
6th International Workshop on Radiative Properties
of Hot Dense Matter

October 31 - November 4, 1994
Sarasota, Florida

January 18, 1995

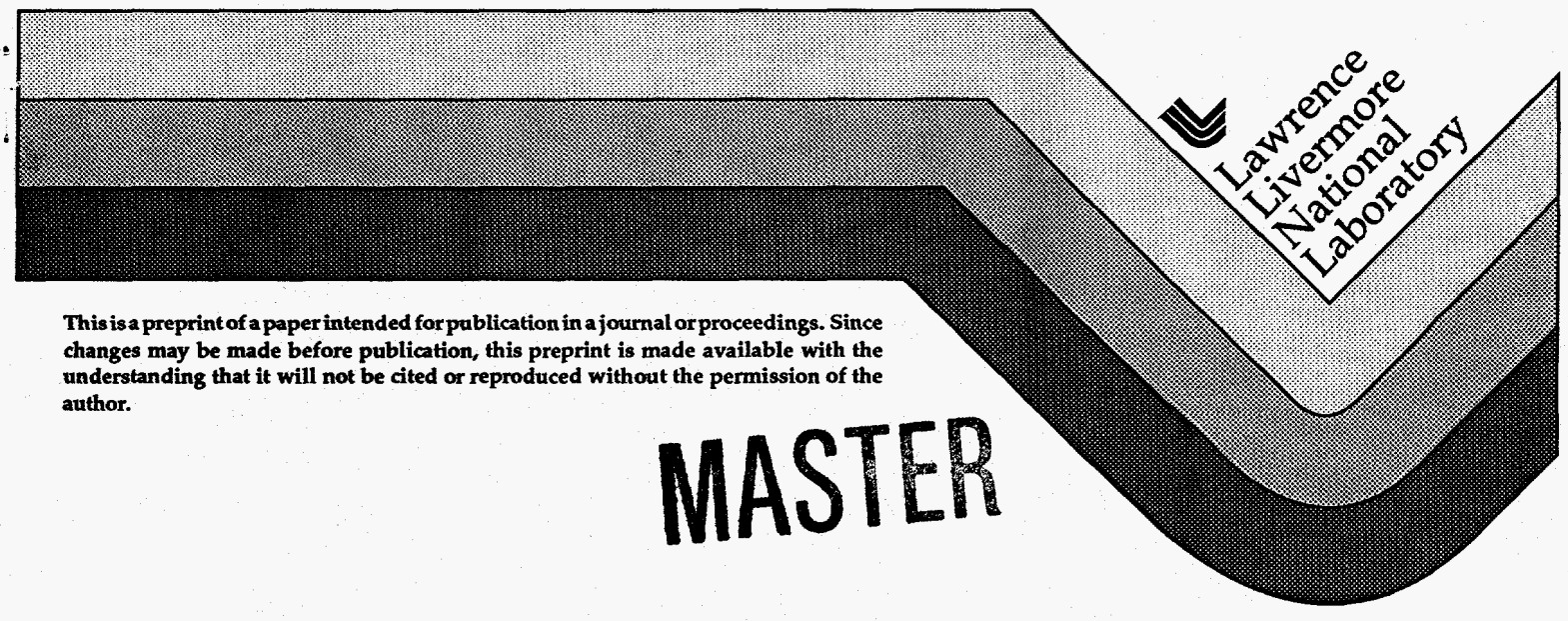

DISCLAIMER

Insights on the Local Density Approximation Plasma Polarization Shift as provided by the Optimum Potential Method

Brian G. Wilson
David A. Liberman
Lawrence Livermore National Laboratory
Livermore Ca

Abstract

The plasma polarization shift computed with a Local Density Functional model of an ion-sphere model is compared with results calculated using an optimum central field effective exchange potential. Indications are that the bulk of the shift is an artifact of the approximate exchange functional describing the interaction between bound and continuum orbitals in the LDA.

I. Introduction

In a recent publication[1] it was shown how the Local Density Functional Approximation (LDA) treatment of exchange could lead to errors in transition energies in spectral regions accessible by opacity experiments. In order to more accurately model these transition arrays, the Optimum Potential Method (OPM) of Talman and Shadwick[2] was advanced as a viable alternative for generating atomic data bases used in opacity calculations. In the OPM, the configuration average (hyper-Hartree-Fock)[3] total energy

$$E^{HF} = \sum_i n_i E_i^o + \frac{1}{2}\sum_i n_i\left(n_i - 1\right)E^{ii} + \frac{1}{2}\sum_{i\neq j} n_i n_j E^{ij}$$

Eqn(1)

where

$$E_i^o \equiv \left\langle i\left|-\nabla^2 - \frac{2Z}{r}\right|i\right\rangle_{avg} = \int_0^\infty dr\, P^*_{n_i l_i}(r)\left\{-\frac{\partial^2}{\partial r^2} + \frac{l_i(l_i+1)}{r^2} - \frac{2Z}{r}\right\}P_{n_i l_i}(r)$$

Eqn(2)

$$E^{ii} = F^0(ii) - \frac{2l_i+1}{4l_i+1}\sum_{k>0}\begin{pmatrix} l_i & k & l_i \\ 0 & 0 & 0\end{pmatrix}^2 F^k(ii)$$

Eqn(3)

$$E^{ij} = F^0(ij) - \frac{1}{2}\sum_k\begin{pmatrix} l_i & k & l_j \\ 0 & 0 & 0\end{pmatrix}^2 G^k(ij)$$

Eqn(4)

is variationally extremized under the constraint that the wavefunctions arise from a single central potential[4]:

$$\frac{\delta E^{HF}}{\delta V(\vec{r})} = \sum_\alpha \int d\vec{r}\,' \frac{\delta E^{HF}}{\delta \Psi_\alpha(\vec{r}\,')}\frac{\delta \Psi_\alpha(\vec{r}\,')}{\delta V(\vec{r})} = 0$$

Eqn(5)

$$-\nabla^2\Psi_\alpha + V(\vec{r})\Psi_\alpha = \varepsilon_\alpha\Psi_\alpha$$

Eqn(6)

This approach is similar to the Parametric Potential Method (PPM)[5] employed by the STA code[6], but differs in that the form of the OPM central field potential is wholly unconstrained. The resulting effective exchange potential, defined by the relation

$$V(r) = -\frac{2Z}{r} + \int_0^\infty d\vec{r}\,'\frac{2}{r_>}\rho(r') + V_x(r)$$

Eqn(7)

has three features that are qualitatively different than the exchange potential predicted by the LDA (see Figure 1). It exhibits the correct Coulomb tail for isolated ions, exhibits quantal oscillations (associated with density gradients), and has a zero slope at the nucleus. The OPM total energies are markedly improved over LDA results when compared to Hartree-Fock values.

Implementing the OPM requires only a small additional computational burden over the LDA, consisting of computing the irregular radial waves for the construction of Greens functions and solving an integral equation (approximated as a system of linear equations). In fact this additional burden may be less than the PPM, which must find a minimum in a multiparameter space of exponential fitting functions.

The OPM also fulfills Janak's theorem[7]

$$\frac{\partial E}{\partial n_i} = \varepsilon_i$$

Eqn(8)

where ε_i denotes the wave equation eigenvalues. Janak's theorem allows a quick evaluation of the Taylor series approximation to the total energy, which in turn allows many transition energies (including orbital relaxation effects) to be calculated without doing a separate SCF calculation for each parent/daughter configuration.[8]

The OPM has previously been employed only for isolated ion calculations. In this paper we shall present a preliminary investigation of the effect of continuum electrons, and specifically use the results to test predictions of the Plasma Polarization Shift computed with the LDA.

The LDA Ion Sphere Model in the Uniform free electron charge Approximation

A common description of a plasma is that of an ensemble of non-interacting ion spheres, with the radius of each sphere determined by the condition that the potential vanishes on the surface, and with the mean free electron density determined by the ensemble average[9]. A further approximation, albeit crude (but widely used due to the computational simplifications that ensue), is that the free electrons form a uniform charge density. In this model[10], the LDA expression to the total energy is formally the same as for an isolated ion

$$E = K - Z\int_0^\infty d\vec{r}\,\frac{\rho(\vec{r})}{r} + \frac{1}{2}\int_0^\infty\int_0^\infty d\vec{r}\,d\vec{r}'\,\frac{\rho(\vec{r})\rho(\vec{r}')}{|\vec{r}-\vec{r}'|} - \frac{3}{4\pi}\int_0^\infty d\vec{r}\,\rho(\vec{r})\left\{3\pi^2\rho(\vec{r})\right\}^{1/3}$$

Eqn(9)

but with ρ denoting the total charge density.

$$\rho(r) = \rho_B(r) + \rho_F(r) = \sum_{i\in B} n_i|\Psi_i(r)|^2 \quad + \quad \begin{cases}\rho_F & r \le R \\ 0 & r > R\end{cases}$$

Eqn(10)

The first term in Eqn(9) denotes the spherical average expectation value of the kinetic energy ("K"), the second term the electron nuclear attraction energy, the second term the classical electron-electron repulsion energy, and the last the electron-electron exchange energy[11]. Note that counter terms were added and subtracted to the Hartree-Fock direct and exchange energy terms to define the LDA exchange energy functional[12]. The LDA system of equations are obtained by requiring stationarity of the total energy with respect to variations in the wavefunction (subject to normalization)

$$\left\{-\frac{1}{2}\nabla^2 + \frac{Z}{r} + \int d\vec{r}\,\frac{\rho(\vec{r}')}{|\vec{r}-\vec{r}'|} + V_{xc}\right\}\Psi_i = \varepsilon_i\Psi_i \qquad V_{xc}[\rho] \equiv \frac{\delta E_{xc}}{\delta\rho(\vec{r})}$$

$$\rho(\vec{r}) = \frac{1}{4\pi r^2}\sum_i n_i|\Psi_i|^2$$

Eqns(11)

which are then solved in a self-consistent manner.

The linearly dependent "plasma shift" of transition energies with free electron density as computed by the LDA model are exemplified in Figure 2. The specific transition (a 2s => 3p excitation out of the $1s^2 2s^2 2p^6 3s^2 3p^2$ bound configuration of Iron) was chosen because of the large discrepancy in the isolated ion limit (831.43 eV) when compared either to Dirac-Hartree-Fock[13] (856.13 eV) or OPM (855.80 eV) results. Note that one of the orbitals involved in the transition is a highly localized inner core electron, which should be relatively non-influenced by the free electron environment.

In order to analyze the LDA polarization shift results, we decompose the expression for the total energy into three components

$$E = E(B) + E(F) + E(B\cap F)$$

Eqn(12)

according to whether the contribution to the energy terms is solely from bound electrons ("B"), solely from free electrons ("F"), and a

component where the bound electrons interact with the free charge ("B∩F"). Explicitly we define

$$E(B) = \sum_{i\in B} n_i \left\{ \varepsilon_i - \int_0^\infty d\vec{r} |\Psi_i|^2 V_{scf} \right\}$$
$$-Z\int_0^\infty d\vec{r}\,\frac{\rho_B(\vec{r})}{r} + \frac{1}{2}\int_0^\infty\int_0^\infty d\vec{r}d\vec{r}'\,\frac{\rho_B(\vec{r})\rho_B(\vec{r}')}{|\vec{r}-\vec{r}'|} - \frac{3}{4\pi}\int_0^\infty d\vec{r}\rho_B(\vec{r})\left\{3\pi^2\rho_B(\vec{r})\right\}^{1/3}$$

Eqn(13)

$$E(F) = K(F)$$
$$-Z\int_0^R d\vec{r}\,\frac{\rho_F(\vec{r})}{r} + \frac{1}{2}\int_0^R\int_0^R d\vec{r}d\vec{r}'\,\frac{\rho_F(\vec{r})\rho_F(\vec{r}')}{|\vec{r}-\vec{r}'|} - \frac{3}{4\pi}\int_0^R d\vec{r}\rho_F(\vec{r})\left\{3\pi^2\rho_F(\vec{r})\right\}^{1/3}$$

Eqn(14)

$$E(B\cap F) = +\frac{1}{2}\int_0^\infty\int_0^R d\vec{r}d\vec{r}'\,\frac{\rho_B(\vec{r})\rho_F(\vec{r}')}{|\vec{r}-\vec{r}'|} + E_{xc}(B\cap F)$$

Eqn(15)

This decomposition is unambiguous for the kinetic and electron-nuclear energy terms (being one body operators) as well as for the classical coulomb repulsion term. However the exchange energy functional, being non-linear in charge density, was arbitrarily split in a judicious manner. The motivation for the particular choice is two-fold. First, the total energy for the bound charge sector should reduce to the expression for the isolated ion limit. Second, the functional form for the exchange energy of the free charge density should be an excellent approximation, for the functional form was derived to be exact in the limit of a uniform free electron gas system.

In a sense the major approximation made for plasma systems is in the remaining term for the exchange energy functional involving bound with free charge. In the LDA we assume it is

$$E_{xc}(B\cap F) = E_{xc}^{LDA}(\rho) - E_{xc}^{LDA}(\rho_F) - E_{xc}(\rho_B)$$

Eqn(16)

The numerical values for each component of each sector is provided in Tables 1 and 2.

Note that with the assumption of uniform free charge density we have exactly

$$E(F) = K(F) - Z\frac{3Q_F}{2R} + \frac{3Q_F^2}{5R} + E_{xc}(F) \quad Q_F \equiv \frac{4}{3}\pi R^3\rho_F$$

Eqn(17)

where Qf is the total free charge in the ion sphere. Obviously the free charge sector cancels in computing transition energies (for

excitations of a given ionization stage) and so is irrelevant to the plasma shift.

The LDA total energy arising from the bound charge sector can now be directly compared with OPM evaluations of the total energy under the following trivial modification. The effect of continuum electrons are now included in the OPM self-consistent system of equations by adding to the nuclear potential an external potential of the form

$$V_{ext}(r) = \frac{(Z^*+1)}{2R}\left\{3-\left(\frac{r}{R}\right)^2\right\} \quad \frac{4}{3}\pi R^3 \rho_F = Z^*+1$$

$$\frac{4}{3}\pi R^3 \rho_F = Z^*+1$$

Eqns(18)

due to the uniform free charge distribution.

Two objections could be raised at this point to the correspondence between the LDA bound charge sector energy and the modified OPM energy. First, note that the OPM cell radius is determined by Z^*+1 in order to cancel the coulomb tail, which is due to a proper treatment of exchange. It should be remembered that in the OPM the potential V(r) is that felt by the 'N'-th indistinguishable bound electron as it is removed to infinity. In contrast, the LDA cell radius is determined by charge neutrality of the ion sphere as felt by an external test charge. The disparities of the two approaches should manifest themselves more strongly for weakly ionized systems.

Second, the LDA bound energy sector is evaluated with wavefunctions formed in a self-consistent potential that treated exchange effects of the continuum electrons with the bound. In the OPM only exchange effects amongst bound electrons were incorporated into the potential generating the wavefunctions. However this turns out not to be a problem, as the bound sector energy value is determined by regions of the wavefunction that are insensitive to the omission of $E_{XC}(B \cap F)$ in determining the potential. This was verified by re-calculating the LDA self-consistent field with those terms turned off.

Despite these reservations a comparison between the LDA bound charge sector energy and the modified OPM energy should still be considered meaningful. This is because both are approximations to the same underlying physics, namely the contribution to the Hartree-Fock energy arising solely from bound wavefunctions in the presence of continuum electrons.

Figures 3(a) and 3(b) present such a comparison for the initial and final configurations in the transition array of Figure 2. The striking feature (aside from the discrepancy in the isolated ion limit due to the inadequate LDA treatment of exchange) is that the OPM results are density independent, in contrast to the LDA. This is true even though plasma effects are significant, as evinced by the perturbation of the eigenvalues with density (see Figure 4), or as seen from the individual components (kinetic, nuclear attraction, Coulomb, and exchange) of the bound energy sector (see Figure 5), which implies a perturbation on the bound charge density.

One intriguing aspect of Figure 5 is that the changes in the kinetic plus direct Coulomb energies cancel the changes in electron-nuclear energies with density. This suggests a possible underlying scaling symmetry to the OPM analogous to the derivation of the virial theorem for non-relativistic systems. The density independence of the OPM bound sector exchange energy is a second surprising result. A theoretical understanding of both features is currently open to investigation.

In spite of the density dependence of the LDA bound charge sector energy for the initial and final configurations, the transition energy arising from this sector remains relatively independent of density (See Figure 6). The plasma shift to the transition energy must therefore be ascribed to the B∩F energy sector, and in that sector the direct Coulomb repulsion is approximately constant as

$$\frac{1}{2}\int_0^{\infty}\int_0^{R} d\vec{r}d\vec{r}' \frac{\rho_B(\vec{r})\rho_F(\vec{r}')}{|\vec{r}-\vec{r}'|} \approx \frac{1}{2}\int_0^{\infty}\int_0^{R} d\vec{r}d\vec{r}' \frac{Q_B\delta(\vec{r})\rho_F(\vec{r}')}{|\vec{r}-\vec{r}'|} = \frac{3Q_BQ_F}{2R}$$

Eqn(19)

holds true to within a fraction of a percent for all cases presented here. Therefore the entire origin of the plasma shift can be attributed to the functional describing the exchange energy between bound and free charge. This in itself is a surprising result, considering the relatively small value this component makes to the total energy calculation.

Summary

Of course rigorous conclusions can not be drawn from the numerical comparisons presented here, but nevertheless they are supportive of certain hypothesis.

The first is that in the LDA, the plasma polarization shift is due to the functional form approximating the exchange energy between bound electrons and free charge. This impacts primarily an

operational definition of a self-consistent field formalism, and has limited physical insight, because after all the distinction between direct Coulomb and Exchange energies in the LDA is somewhat artificial.

Second, because the LDA transition energy differs from the OPM in the isolated ion limit (the latter being close to Hartree-Fock), and the LDA density dependence of the bound energy differs from the OPM, there is no reason to believe the density dependence of the LDA B∩F exchange energy functional. Furthermore, based on the surprising density independence of the OPM bound charge exchange, it might be expected that an accurate model would exhibit no density dependence of the B∩F exchange, and hence no plasma polarization shift. Certainly the exchange energy is not a functional of the total charge density, which is directly altered by continuum electrons, but of the shape of the wavefunctions which underlay the construction of a charge density. The latter are much more insensitive to perturbation, and would have to be preferentially changed between the initial and final configurations of a transition to produce a plasma shift.

Work at LLNL was performed under the auspices of the U.S. Department of Energy, Contract No. W-7405-Eng-48.

Figure Captions.

Figure 1: The central field effective exchange potential computed by the OPM method as compared with the LDA result (top). The quantum oscillations of the OPM are correlated with extrema of the dimensionless density gradient parameter (bottom).

Figure 2: LDA transition energies for the $1s^2 2s^2 2p^6 3s^2 3p^2$ to $1s^2 2s^1 2p^6 3s^2 3p^3$ excitation of Iron, showing the linear in density plasma shift. The free electron number density range corresponds to aproximately 0.1 to normal solid density in Iron.

Figure 3: LDA and OPM bound charge sector total energies for Iron as a function of free electron density. On the left is the initial $1s^2 2s^2 2p^6 3s^2 3p^2$ configuration, at right the final $1s^2 2s^1 2p^6 3s^2 3p^3$ configuration.

Figure 4: OPM orbital eigenvalues versus free electron density. The eigenvalues are parametrized in the form of an effective Z using hydrogenic scaling.

Figure 5: OPM bound charge sector energies by component (i.e. electron-nuclear attraction, exchange, direct Coulomb repulsion, and kinetic energy contributions) for the initial configuration.

Figure 6: The LDA transition energy as a function of density, showing that portion of the plasma shift arising from contributions arising solely from bound charge.

---

[1]B. G. Wilson, David A. Liberman, & Paul T. Springer, "A Deficiency of Local Density Functionals for the Calculation of Self-Consistent Field Atomic Data in Plasmas", submitted to J.Q.S.R.T. (Oct 27,1994)

[2]J. Talman, W. Shadwick, Phys.Rev. A14, p.36 (1976), J. Talman, Comp.Phys. Commun. 54, p.85 (1989), ibid., p.95.

[3]J. C. Slater, J. Wood, Int. J. Quant. Chem. 4,p.3 (1971)

---

[4]For simplicity of presentation we have written the non-relativistic / Schroedinger equation limit. The relativistic generalization is straightworward and was employed in calculating the results of this paper.

[5]M. Klapisch, Comput.Phys.Commun.2, p.269 (1971); M.Klapisch, J.Schwob, B.Fraenkel, and J.Oreg, J.Opt.Soc.Am.67, p.148 (1977)

[6]A. Bar-Shalom et al, Phys.Rev.40, p.3183 (1989); "Calculation of Emision and Absorption Spectra of LTE Plasm by the STA method", A. Bar-Shalom, J.Oreg and W. Goldstein, in 'Radiative Properties of Hot Dense Matter', ed. W. Golstein, C. Hooper, J. Gautier, J. Seely, and R.Lee, World Scientific (1990)

[7]J. Janak, Phys.Rev.B18, p.7165 (1978)

[8]D. Liberman, J. Albritton, "Rapid Calculations of Properties of Plasma Atoms and Ions", UCRL-50021-84 (Lawrence Livermore National Laboratory Laser Program Annual Report 84) pp.3-66, (1984)

[9]D. Liberman, Phys.Rev. B20, p.4981 (1979), "INFERNO", Los Alamos Manual LA-10309-M (1985)

[10]D. Liberman, D.Cromer, J. Waber, Comput. Phys.Commun.2, p.107 (1971)

[11]For notational simplicity we write the basic Kohn-Sham form for the exchange energy functional. For actual calcualtions the Gunnarsson-Lundqvist form of the exchange-correlational energy functional was employed. For a more detailed description of the functional see O.Gunnarsson, b.Lundqvist, Phys.Rev.B13, p.4274 (1976).
To test the sensity of the results to the specific choice of correlational functional, calculations were re-run with the bare Kohn-Sham exchange functional. No qualitative changes in the results presented here were obtained.

[12]I. Lindgren, A. Rosen, Case Studies in Atomic Physics 4, p.93 (1974)

[13] K. Dayall et al, Comput.Phys.Commun.55, p.425 (1989)

Figure 1

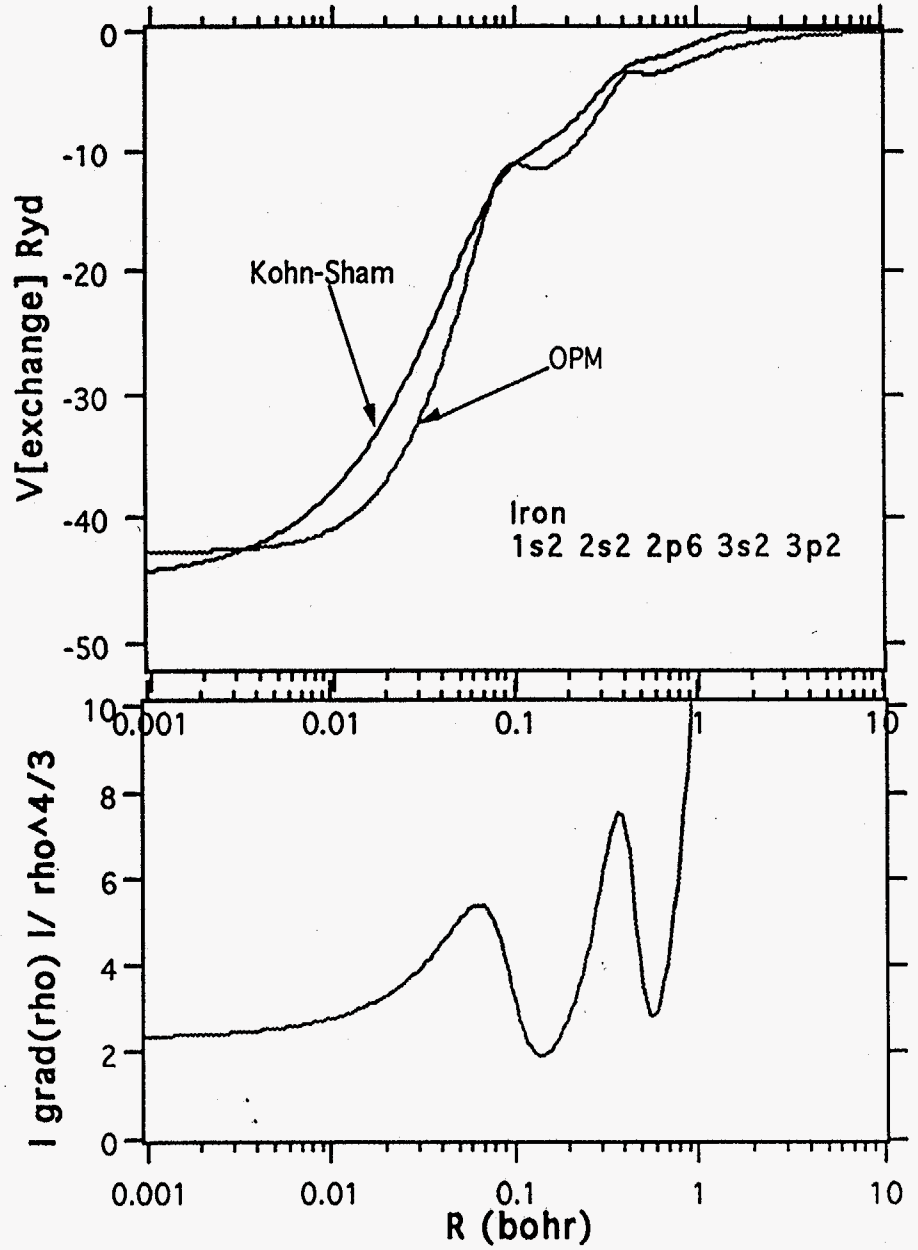
V[exchange] Ryd
0
-10
-20
-30
-40
-50
Kohn-Sham
OPM
Iron
1s2 2s2 2p6 3s2 3p2
0.001
0.01
0.1
1
10
I grad(rho) I/ rho^4/3
8
6
4
2
0
R (bohr)

Figure 2

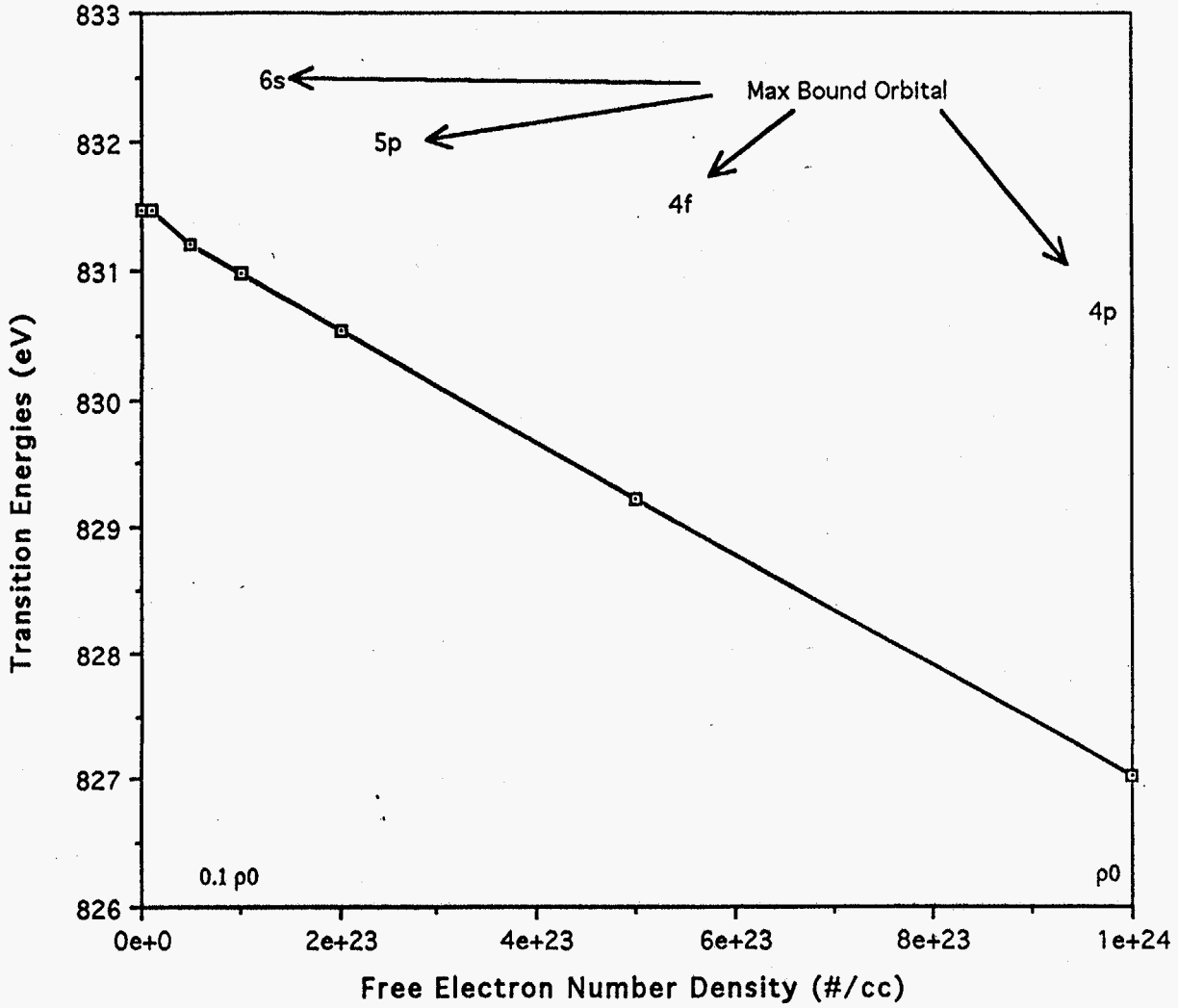
833
832
831
830
829
828
827
826
Transition Energies (eV)
6s
5p
4f
Max Bound Orbital
4p
0.1 ρ0
ρ0
0e+0
2e+23
4e+23
6e+23
8e+23
1e+24
Free Electron Number Density (#/cc)

Figure 3

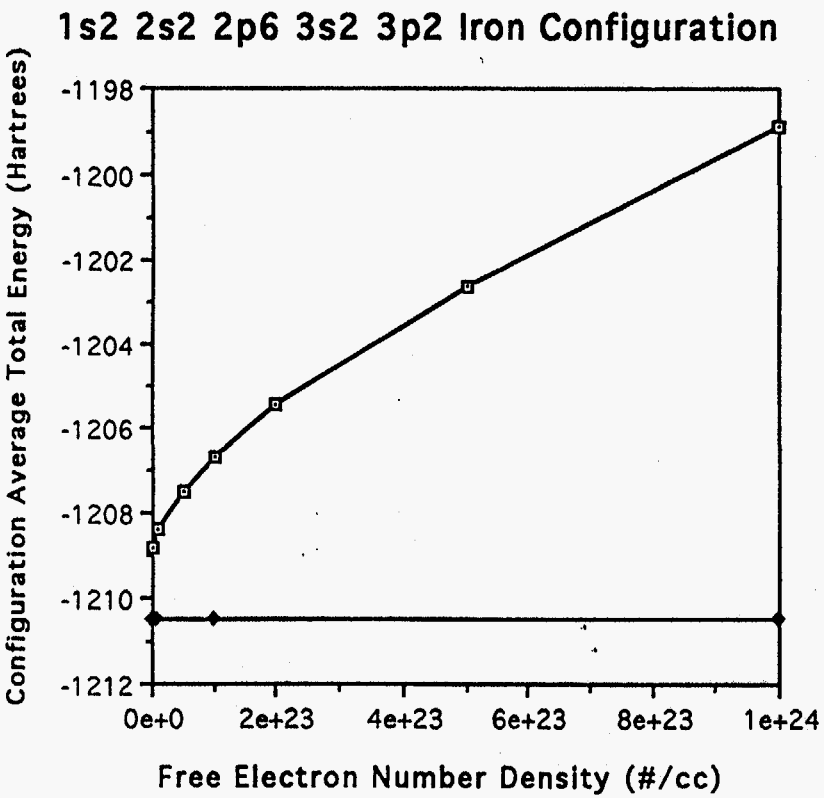
1s2 2s2 2p6 3s2 3p2 Iron Configuration
Configuration Average Total Energy (Hartrees)
-1198
-1200
-1202
-1204
-1206
-1208
-1210
-1212
0e+0
2e+23
4e+23
6e+23
8e+23
1e+24
Free Electron Number Density (#/cc)

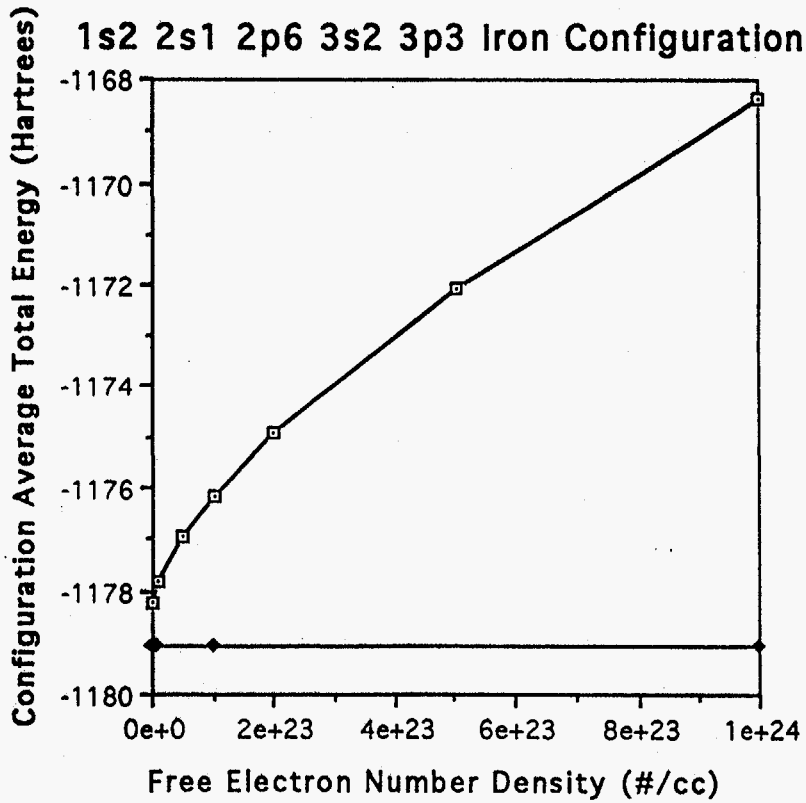
1s2 2s1 2p6 3s2 3p3 Iron Configuration
Configuration Average Total Energy (Hartrees)
-1168
-1170
-1172
-1174
-1176
-1178
-1180
0e+0
2e+23
4e+23
6e+23
8e+23
1e+24
Free Electron Number Density (#/cc)

Figure 4

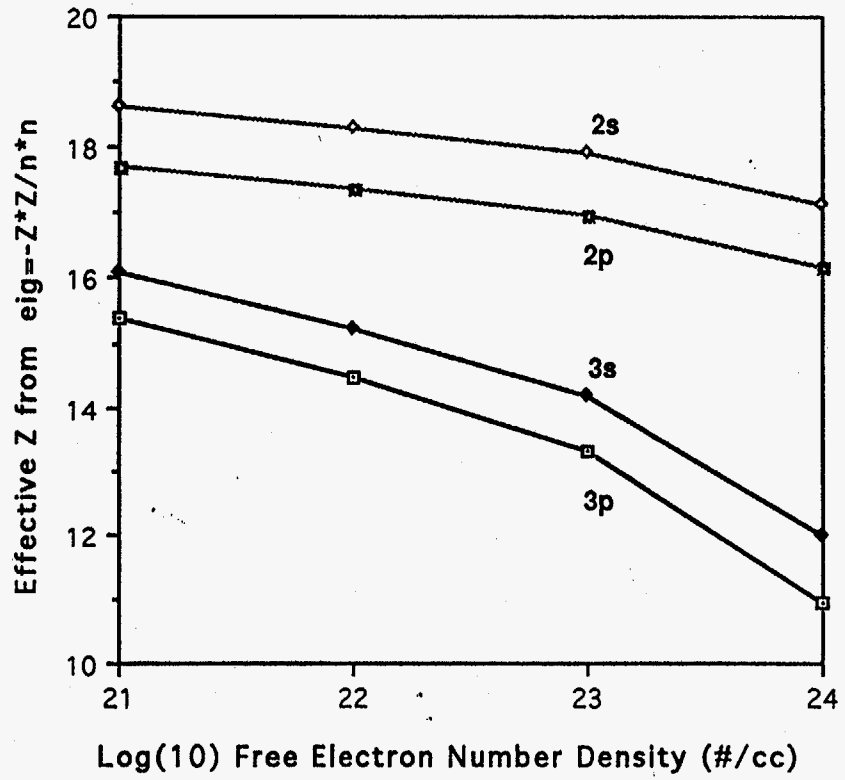
20
18
16
14
12
10
21
22
23
24
2s
2p
3s
3p
Effective Z from eig=-Z*Z/n*n
Log(10) Free Electron Number Density (#/cc)

Figure 5

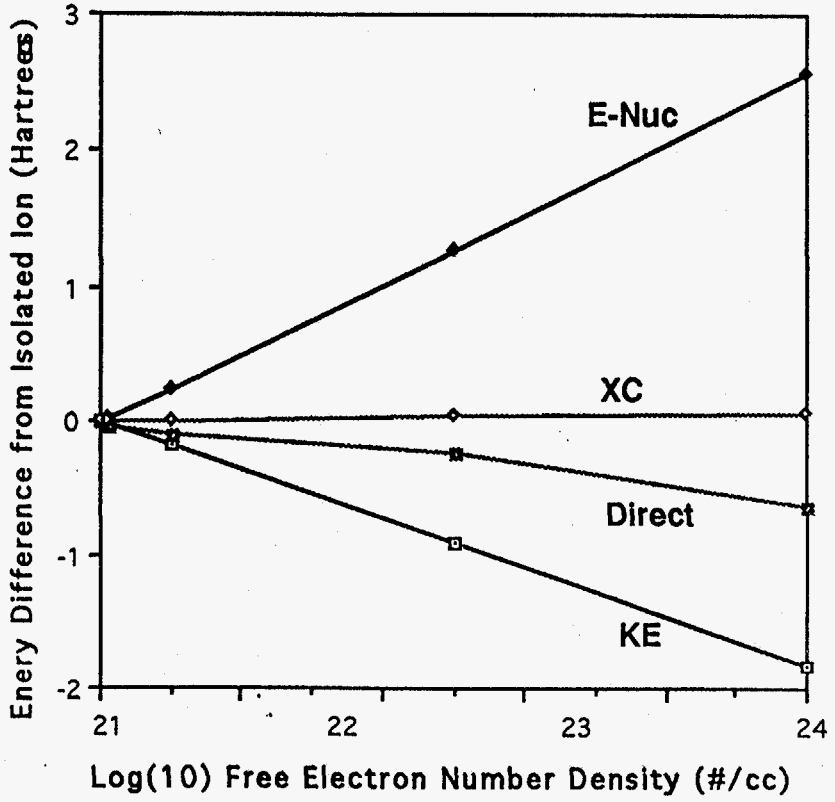
Enery Difference from Isolated Ion (Hartrees)
3
2
1
0
-1
-2
21
22
23
24
Log(10) Free Electron Number Density (#/cc)
E-Nuc
XC
Direct
KE

Figure 6

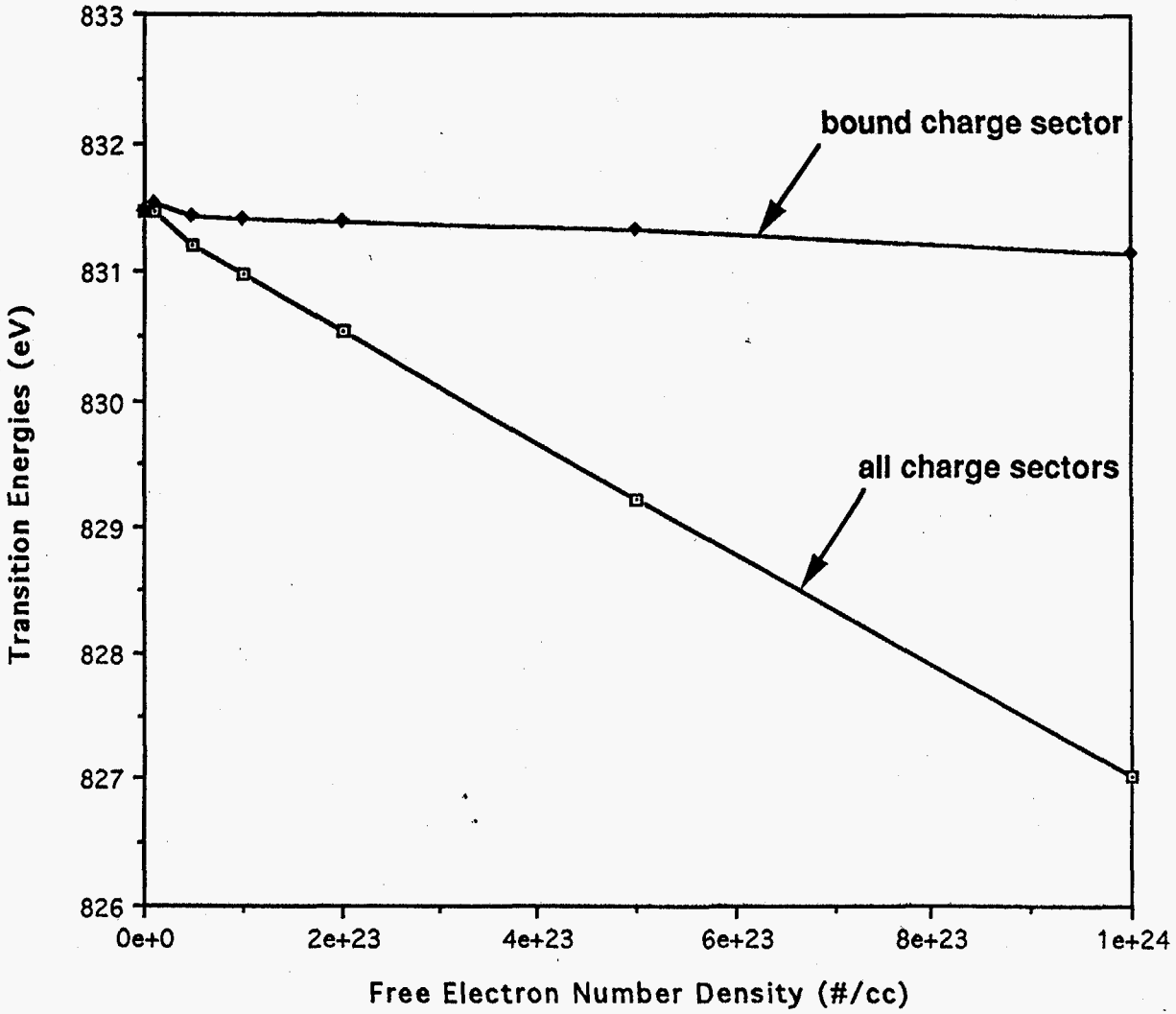
833
832
831
830
829
828
827
826
Transition Energies (eV)
bound charge sector
all charge sectors
0e+0
2e+23
4e+23
6e+23
8e+23
1e+24
Free Electron Number Density (#/cc)

Table 1

LDA Energies (in Hartrees) for the configuration $1s^2 2s^2 2p^6 3s^2 3p^2$ of Iron as a function of continuum electron density (grouped by BB,FF, B∩F charge sectors).

	0	1e+22	5e+22	1e+23	2e+23	5e+23	1e+24
KE	+1226.1657	+1226.5859	+1227.3600	+1228.0066	+1229.0044	+1231.0927	+1233.4927
E-Nuc	-2707.8359	-2707.8052	-2707.6778	-2707.5178	-2707.1923	-2706.1965	-2704.5114
Direct	+316.0669	+316.0593	316.0273	+315.9866	+315.9055	+315.6591	+315.2356
Exc	- 43.1948	- 43.1941	-43.1911	- 43.1874	-43.1799	-43.1569	-43.1176
Total	-1208.7980	-1208.3552	-1207.4816	-1206.7120	-1205.4623	-1202.6016	-1198.9007
E-Nuc *		-37.5692	-64.2398	-80.9409	-101.9786	-138.4001	-174.3796
Direct *		+6.9361	+11.8596	+14.9440	+18.8268	+25.5504	+32.1923
Exc		-1.3820	-2.2405	-2.7577	-3.39534	-4.4751	-5.5216
Direct		20.2208	34.5466	43.4954	54.7356	74.0809	93.0045
Exc		-0.0114	-0.0471	-0.0859	-0.1546	-0.3290	-0.5737
Total	-1208.7980	-1220.1610	-1227.6029	-1232.0566	-1237.4266	-1246.1745	-1254.1787
Σeigs	- 906.7138	- 886.5013	-872.1956	- 863.2785	-852.0882	-832.9082	-814.2681
r_{cell}	∞	12.457	7.2852	5.7820	4.5892	3.3815	2.6838

Table 1a

OPM Energies (in Hartrees) for the configuration $1s^2 2s^2 2p^6 3s^2 3p^2$ of Iron as a function of continuum electron density (BB charge sector only).

	0	1e+22	1e+23	5.e+23	1e+24
KE	+1229.0406	+1229.0236	+1228.8631	+1228.1417	+1227.2183
E-Nuc	-2710.8347	-2710.8115	-2710.5862	-2709.5705	-2708.2621
Direct	+316.0669	+316.2325	+316.1618	315.8422	+315.4286
Exc	-44.9318	-44.9312	-44.9251	-44.8979	-44.8627
Total	-1210.4866	-1210.4666	-1210.4865	-1210.4845	-1210.4780
Σeigs	-916.9387	-895.3982	-870.9289	-839.0672	-825.2454
r_{cell}	∞	12.7943	5.9386	3.4729	2.7565

Table 2

LDA Energies (in Hartrees) for the configuration $1s^2 2s^1 2p^6 3s^2 3p^3$ of Iron as a function of continuum electron density (grouped by BB,FF, B∩F charge sectors).

	0	1e+22	5e+22	1e+23	2e+23	5e+23	1e+24
KE	+1194.6020	+1195.0238	+1195.7859	+1196.4338	+1197.3998	+1199.4264	+1201.7209
E-Nuc	-2629.8588	-2629.8270	-2629.6875	-2629.5116	-2629.1625	-2628.0882	-2626.2703
Direct	+298.3957	+298.3872	298.3524	+298.3082	+298.2195	+297.9509	+297.4896
Exc	- 41.3826	- 441.3819	-41.3785	- 41.3743	-41.3661	-41.3405	-41.2969
Total	-11178.2437	-1177.7975	-1176.9277	-1176.1439	-1174.9093	-1172.0514	-1168.3567
E-Nuc *		-37.5692	-64.2398	-80.9409	-101.9786	-138.4001	-174.3796
Direct *		+6.9361	+11.8596	+14.9440	+18.8268	+25.5504	+32.1923
Exc		-1.3820	-2.2405	-2.7577	-3.3953	-4.4751	-5.5216
Direct		20.2196	34.5410	43.4842	54.7131	74.0245	92.8908
Exc		-0.0118	-0.0494	-0.0904	-0.1633	-0.3492	-0.6113
Total	-1178.2437	-1189.6052	-1197.0569	-1201.5057	-1206.9050	-1215.7011	-1223.7860
Σeigs	- 893.2357	- 873.0283	-858.7269	- 849.8133	-838.6485	-819.5266	-800.9845
r_{cell}	∞	12.457	7.2852	5.7820	4.5892	3.3815	2.6838

Table 2a

OPM Energies (in Hartrees) for the configuration $1s^2 2s^1 2p^6 3s^2 3p^3$ of Iron as a function of continuum electron density (BB charge sector only).

	0	1e+22	1e+23	1e+24
KE	+1196.5747	+1196.5558	+1196.3747	+1194.5214
E-Nuc	-2631.7945	-2631.7680	-2631.5155	-2628.9151
Direct	298.3847	298.3764	298.2984	297.4918
Exc	-42.2382	-42.2374	-42.2308	-42.1618
Total	-1179.0733	-1179.0733	-1179.0732	-1179.0637
Σeigs	-903.2736	-881.7574	-857.3011	-808.1192
r_{cell}	∞	12.79432	5.9386	2.7565